Constraining hadronization mechanisms with + c /D0 production ratios in Pb–Pb collisions at √sNN = 5.02 TeV

(ALICE Collaboration) Acharya, S.; ...; Erhardt, Filip; ...; Gotovac, Sven; ...; Jerčić, Marko; ...; Karatović, David; ...; ...

Constraining hadronization mechanisms with Λ_c^+/D^0 production ratios in Pb–Pb collisions at $\sqrt{s_{NN}} = 5.02$ TeV

ALICE Collaboration [*]

ARTICLE INFO

ABSTRACT

The production of prompt Λ_c^+ baryons at midrapidity ($|y| < 0.5$) was measured in central (0–10%) and mid-central (30–50%) Pb–Pb collisions at the center-of-mass energy per nucleon–nucleon pair $\sqrt{s_{NN}} =$ 5.02 TeV with the ALICE detector. The results are more precise, more differential in centrality, and reach much lower transverse momentum ($p_T = 1$ GeV/c) with respect to previous measurements performed by the ALICE, STAR, and CMS Collaborations in nucleus–nucleus collisions, allowing for an extrapolation down to $p_T = 0$. The p_T-differential Λ_c^+/D^0 ratio is enhanced with respect to the pp measurement for $4 < p_T < 8$ GeV/c by 3.7 standard deviations (σ), while the p_T-integrated ratios are compatible within 1σ. The observed trend is similar to that observed in the strange sector for the Λ/K_S^0 ratio. Model calculations including coalescence or statistical hadronization for charm-hadron formation are compared with the data.

1. Introduction

Heavy-ion collisions at LHC energies produce a phase of strongly-interacting matter, known as the quark–gluon plasma (QGP), in which quarks and gluons are deconfined [1]. The existing measurements indicate that the QGP behaves as a strongly-coupled low-viscosity liquid-like system [2]. Heavy quarks, produced at the start of the collision, experience the full evolution of the system and constitute a unique probe of the QGP properties [3]. The hadronization of heavy quarks into open heavy-flavor hadrons is expected to be influenced by the presence of a deconfined medium. Theoretical calculations that include modified hadronization via quark coalescence or via a resonance recombination approach [4–9] predict a significant enhancement of the Λ_c^+/D^0 yield ratio in heavy-ion collisions compared to the expected ratio in pp collisions. In addition, the collective radial expansion of the system determines a flow-velocity profile common to all thermalized particles, that could increase the Λ_c^+/D^0 ratio at intermediate transverse momentum, i.e. $2 \lesssim p_T \lesssim 8$ GeV/c [7,8,10]. The study of such a potential enhancement requires a good understanding of Λ_c^+ production in smaller collision systems, which showed surprising features at LHC energies. The production of Λ_c^+ baryons was measured at the LHC in pp collisions by the ALICE Collaboration at $\sqrt{s} = 5.02$, 7, and 13 TeV [11–14], by the CMS Collaboration at 5.02 TeV [15], and by the LHCb Collaboration at 7 TeV [16].

At midrapidity, the ALICE and CMS results show a significant enhancement in the Λ_c^+/D^0 yield ratio (up to a factor 2–5 for $p_T < 8$ GeV/c) compared to e^+e^- and e^-p measurements [17–22] and QCD-inspired theoretical predictions [23–26] where charm fragmentation is tuned on e^+e^- and e^-p measurements [27,28]. Models that introduce new color-reconnection topologies in string fragmentation [29] or hadron production via coalescence [30] as well as models that are based on statistical hadronization including feed-down from unobserved charm-baryon states [31] are able to describe the Λ_c^+/D^0 ratio at midrapidity. The values of the Λ_c^+/D^0 ratio measured at forward rapidity by the LHCb Collaboration are smaller than those at midrapidity, indicating a non-negligible rapidity dependence.

A recent measurement performed by ALICE in intervals of charged-particle multiplicity dN_{ch}/dη in pp collisions at $\sqrt{s} = 13$ TeV [32] showed that in a hadronic collision, even at relatively small multiplicities, charm-quark hadronization proceeds differently than in e^+e^- collisions. The p_T-dependence of the Λ_c^+/D^0 ratio evolves with multiplicity and the maximum of the ratio increases for the higher multiplicity intervals, while the p_T-integrated Λ_c^+/D^0 ratios do not show a significant dependence on multiplicity up to $\langle$dN_{ch}/d$\eta\rangle \approx 40$. Whether the p_T-differential Λ_c^+/D^0 ratio keeps evolving with multiplicity up to the typical multiplicities of Pb–Pb collisions, and whether an overall p_T-integrated enhancement of Λ_c^+ production relative to the D^0 one is present at higher multiplicities, as proposed by coalescence models including light diquark states [4,5,9], are open questions and fundamental to the understanding of charm-quark hadronization.

[*] E-mail address: alice-publications@cern.ch.

The Λ_c^+ production in nucleus–nucleus collisions was measured for the first time at the LHC by ALICE in Pb–Pb collisions at $\sqrt{s_{NN}} = 5.02$ TeV in the 0–80% centrality interval for $6 < p_T < 12$ GeV/c [33]. The Λ_c^+/D^0 ratio was found to be close to unity, larger than the corresponding ratio measured in pp collisions, and well described by calculations including hadronization via coalescence mechanisms [7,8]. The Λ_c^+/D^0 ratio measured in the interval $3 < p_T < 6$ GeV/c by the STAR Collaboration in Au–Au collisions at $\sqrt{s_{NN}} = 200$ GeV [34] shows an increasing trend towards more central collisions and is also described by model calculations including hadronization via coalescence [5,7,8,35–37]. Considering together the values calculated by STAR in 10–80% Au–Au collisions and by ALICE in pp and p–Pb collisions [11,32] a possible increase of the p_T-integrated Λ_c^+/D^0 ratio at high multiplicity is neither excluded nor confirmed. The CMS measurement in Pb–Pb collisions at $\sqrt{s_{NN}} = 5.02$ TeV [15], performed in the interval $10 < p_T < 20$ GeV/c, is consistent with the pp result within uncertainties as well as with predictions considering only string fragmentation [29], suggesting that coalescence has no significant effect in this p_T range. The production of Λ_c^+ baryons was also measured in p–Pb collisions at $\sqrt{s_{NN}} = 5.02$ TeV by the ALICE and LHCb Collaborations [11,12,38]. The current measurements do, however, not allow to draw conclusions on the role of different cold-nuclear matter effects and the possible presence of hot-medium effects. Recently, LHCb also measured the Λ_c^+/D^0 ratio in peripheral (65–90%) Pb–Pb collisions at $\sqrt{s_{NN}} = 5.02$ TeV, which was observed to be consistent with the LHCb ratio in p–Pb collisions [39].

In this letter, the measurement of the p_T-differential production yields of prompt Λ_c^+ baryons in central (0–10%) and mid-central (30–50%) collisions using the 2018 Pb–Pb at $\sqrt{s_{NN}} = 5.02$ TeV are reported down to $p_T = 1$ GeV/c. The results are more precise and more differential in p_T and centrality with respect to previous measurements [15,33,34]. The Λ_c^+/D^0 yield ratios and the nuclear modification factor R_{AA}, which is defined as the ratio of the production yield in Pb–Pb collisions and the cross section in pp collisions scaled by the average nuclear overlap function $\langle T_{AA} \rangle$ (proportional to the number of nucleon–nucleon collisions), are reported as function of p_T and compared with theoretical predictions. The p_T-integrated Λ_c^+ production yield and Λ_c^+/D^0 ratio, extrapolated to $p_T = 0$, are also presented for the first time in Pb–Pb collisions.

2. Experimental apparatus and data sample

The ALICE apparatus is described in detail in [40,41]. The data were collected using triggers based on the signal in the V0 detectors [42]. A minimum bias trigger, which required coincident signals in both detecting components of the V0 detector along the beam axis on opposite sides of the interaction point, was exploited. In addition, and differently with respect to the previous Pb–Pb data taking period at the same $\sqrt{s_{NN}}$, two new trigger selections were introduced to enrich the sample of central and mid-central collisions via an online event selection based on the V0-signal amplitude. Events were further selected offline using timing information from the V0 detectors and the neutron Zero Degree Calorimeters [43] to reject events due to the interaction of one of the beams with residual gas in the vacuum tube. Furthermore, only events with a primary vertex reconstructed within ±10 cm from the center of the detector along the beam axis were considered in the analysis. Collisions were classified into centrality intervals, defined in terms of percentiles of the hadronic Pb–Pb cross section, using the V0-signal amplitudes [44]. The number of events in the centrality classes 0–10% and 30–50% considered for this analysis is about 100×10^6 and 85×10^6, respectively, corresponding to a luminosity of (130.5 ± 0.5) μb^{-1} and (55.5 ± 0.2) μb^{-1} [45].

The Monte Carlo (MC) simulations utilized in this analysis were obtained using the HIJING 1.36 event generator [46] to simulate Pb–Pb collisions at $\sqrt{s_{NN}} = 5.02$ TeV. In each simulated event, Λ_c^+ signals were added by injecting $c\bar{c}$ or $b\bar{b}$ pairs generated with the PYTHIA 8.243 event generator [23] with the Monash tune [47]. The Λ_c^+ baryons were forced to decay into the hadronic decay channel of interest, $\Lambda_c^+ \to pK_S^0$ followed by $K_S^0 \to \pi^+\pi^-$, using PYTHIA. All generated particles were transported through the ALICE detector using the GEANT3 package [48]. The conditions of all the ALICE detectors in terms of active channels, gain, noise level, and alignment, and their evolution with time during the data taking, were taken into account in the simulations.

3. Data analysis

The Λ_c^+ baryon and its charge conjugate were reconstructed by exploiting the topology of the hadronic decay channel $\Lambda_c^+ \to pK_S^0$ (branching ratio BR = 1.59 ± 0.08%), followed by the subsequent decay $K_S^0 \to \pi^+\pi^-$ (BR = 69.20 ± 0.05%) [28]. Charged-particle tracks used to define the Λ_c^+ candidates are reconstructed using the Inner Tracking System (ITS) [49] and the Time Projection Chamber (TPC) [50], located in a solenoid magnet that provides a 0.5 T field parallel to the beam direction. The $\Lambda_c^+ \to pK_S^0$ candidates combine a proton-candidate track with a K_S^0-meson candidate, reconstructed in the $K_S^0 \to \pi^+\pi^-$ decay channel. Only proton (pion) tracks with $|\eta| < 0.8$, $p_T > 0.4$ (0.1) GeV/c, at least 70 out of 159 associated crossed TPC pad rows, a ratio of crossed rows to findable clusters in the TPC larger than 0.8, at least 50 clusters in the TPC available for particle identification (PID), and a χ^2/ndf < 1.25 in the TPC (where ndf is the number of degrees of freedom involved in the track fit procedure) were considered for the analysis. Moreover, a minimum number of two hits (out of six) in the ITS, with at least one in the inner two layers, were required for the proton track. The selection of tracks with $|\eta| < 0.8$ limits the Λ_c^+ acceptance in rapidity. For this reason a fiducial acceptance selection was applied on the rapidity of the Λ_c^+ candidates, $|y_{lab}| < y_{fid}(p_T)$, where y_{fid} increases from 0.6 to 0.8 in $1 < p_T < 5$ GeV/c, and $y_{fid} = 0.8$ for $p_T > 5$ GeV/c.

Unlike the previous analysis based on linear selections [33], the Λ_c^+-candidate selection was performed using multivariate techniques based on the Boosted Decision Tree (BDT) algorithm provided by the XGBoost package [51]. Before the training, loose kinematic and topological selections were applied to the K_S^0-meson candidate together with the particle identification of the proton-candidate track. The PID was performed using the specific ionization energy loss dE/dx in the TPC gas and the time of flight from the interaction point to the Time-Of-Flight (TOF) detector [52,53]. The BDT training was performed considering as signal candidates prompt (not coming from beauty-hadron decays) Λ_c^+ decays from MC simulations. Background candidates were taken from the sidebands of the invariant mass distribution in data (defined to be outside a 80 MeV/c^2 window around the Λ_c^+ mass value reported by the PDG [28]).

The variables that were most important in the training were the PID-related variables of the proton-candidate track, the displacement of the proton-candidate track from the primary vertex, the distance between the K_S^0-meson decay vertex and the primary vertex, and the cosine of the pointing angle between the K_S^0-meson candidate line of flight and its reconstructed momentum vector. Independent BDTs were trained for the different p_T and centrality intervals.

The selection on the BDT output was tuned in each p_T interval to maximize the expected statistical significance, which is estimated using i) the expected signal obtained from FONLL calculations [54,55] scaled by the corresponding $\langle T_{AA} \rangle$ [45] and mul-

tiplied by the BDT selection efficiency and ii) the expected background estimated from an invariant mass sideband fit using a fraction of the data.

After applying selections on the BDT output, the yields of Λ_c^+ baryons were extracted in each p_T interval via binned maximum-likelihood fits to the candidate invariant mass distributions. The fitting function consisted of a Gaussian term to estimate the signal and a second-, third-, or fourth-order polynomial function (depending on the p_T interval) to estimate the background. The default background fitting function was chosen after dedicated studies to obtain a good description of the invariant mass distribution in the sidebands. The other functions were considered for evaluating the systematic uncertainty.

The raw-yield extraction is challenging, especially at low p_T with signal-to-background ratios below one per mille and relative statistical uncertainties on the extracted raw yield varying between 15–35%, as presented in Appendix A. Given the critical signal extraction due to the low signal-to-background ratios, the width of the Gaussian term for the signal was fixed to the value obtained from simulations. It was verified that the widths from the simulation were consistent within uncertainties to those extracted from fits to data without constraints on the width of the Gaussian (with a relative uncertainty of 1–2% in simulation and 20–30% in data). In addition, the stability of the signal extraction was further verified by i) fitting purely background candidates from simulations and ii) by repeating the fit after subtracting a background component estimated with an event-mixing technique. For the latter, the events were grouped in pools based on the primary-vertex position along z and the estimated centrality. For the first study, none of the invariant mass fits allowed to extract a signal in the Λ_c^+ invariant mass region. For the second study, fits to the background-subtracted invariant mass distributions resulted in compatible Λ_c^+ raw yields to the ones extracted from the default fits.

The corrected yields of prompt Λ_c^+ baryons were obtained in each centrality interval as

$$\left.\frac{dN^{\Lambda_c^+}}{dp_T}\right|_{|y|<0.5} = \frac{f_{prompt} \times \frac{1}{2}\left.N_{raw}^{\Lambda_c^\pm}\right|_{|y|<y_{fid}}}{\Delta p_T \times c_{\Delta y} \times (A \times \varepsilon)_{prompt} \times BR \times N_{ev}}. \quad (1)$$

The raw yield values $N_{raw}^{\Lambda_c^\pm}$, extracted in a given p_T interval of width Δp_T, were divided by a factor two and multiplied by the prompt fraction f_{prompt} to obtain the charge-averaged yields of prompt Λ_c^+. Furthermore, they were divided by $c_{\Delta y} \times (A \times \varepsilon)$, enclosing the rapidity coverage and the acceptance-times-efficiency, by the BR of the decay channel, and by the number of analyzed events N_{ev}.

The $(A \times \varepsilon)$ correction was determined from MC simulations, using samples not employed in the BDT training. The generated p_T spectrum used to calculate the efficiencies was reweighted to reproduce the shape obtained from the D^0 measurement [56] multiplied by Λ_c^+/D^0 calculations from the TAMU model [8] in 0–10% and 30–50% Pb–Pb collisions at $\sqrt{s_{NN}} = 5.02$ TeV. The $(A \times \varepsilon)$ increases from 1% (3%) at low p_T to about 12% (16%) at high p_T for central (mid-central) collisions. The correction factor for the rapidity acceptance, $c_{\Delta y}$, was computed as the ratio between the generated Λ_c^+-baryon yield in $\Delta y = 2y_{fid}(p_T)$ and that in $|y| < 0.5$ using the reweighted p_T shape and the rapidity distribution from PYTHIA 8 simulations [23]. It was verified in [56] that for D mesons the calculation of $c_{\Delta y}$ is only weakly sensitive to the rapidity distribution used for its calculation.

The f_{prompt} fraction of the reconstructed signal was estimated using a similar strategy as described in [33]. In particular, the beauty-hadron production cross section was estimated with FONLL

Table 1
Relative systematic uncertainties of the prompt Λ_c^+-baryon corrected yield in Pb–Pb collisions for central and mid-central events in representative p_T intervals.

Centrality interval	0–10%		30–50%	
p_T (GeV/c)	4–6	12–24	1–2	6–8
Yield extraction	11%	17%	14%	12%
Tracking efficiency	10%	9%	12%	8%
Selection efficiency	8%	8%	7%	7%
Prompt fraction	$^{+8}_{-6}$%	$^{+13}_{-13}$%	$^{+4}_{-3}$%	$^{+12}_{-8}$%
MC p_T shape	2%	negl.	2%	1%
Centrality limits	< 0.1%		2%	
Branching ratio	5.5%			
Total syst. unc.	$^{+20}_{-19}$%	$^{+25}_{-25}$%	$^{+21}_{-21}$%	$^{+21}_{-19}$%

calculations [54,55], the fraction of beauty quarks that fragment into Λ_b^0 was estimated from the $\Lambda_b^0/(B^0 + B^+)$ ratio measured by LHCb in pp collisions at $\sqrt{s} = 13$ TeV [57] following the same strategy as used in [11], and the kinematics of the decay of beauty hadrons $H_b \to \Lambda_c^+ + X$ simulated with PYTHIA 8 [23]. The branching ratios were taken as implemented in PYTHIA 8.243, corresponding to approximately 82% for Λ_b^0 baryons and 2% for either B^0, B^+, and B_s^+ mesons. In addition, the f_{prompt} fraction is modified to account for the nuclear modification factor of Λ_c^+ baryons from beauty-hadron decays. The central correction is chosen such that $R_{AA}^{non-prompt} = 2 \times R_{AA}^{prompt}$ as predicted by the "Catania" theoretical calculation [6]. The resulting f_{prompt} fraction was found to be about 0.97 at low p_T and about 0.81 at high p_T.

The systematic uncertainties of the Λ_c^+ corrected yields include contributions from i) the extraction of the raw yield, ii) the tracking efficiency, iii) the Λ_c^+ selection efficiency, iv) the MC generated p_T spectra, v) the statistical uncertainty of the efficiency, and vi) the subtraction of feed-down Λ_c^+ baryons from b-hadron decays. The estimated values of these systematic uncertainties are summarized for representative p_T intervals in Table 1. In addition, a global systematic uncertainty due to the centrality interval definition (2% for mid-central, negligible for central) [56] and the branching ratio (5.5%) [28] was assigned. For the R_{AA} observable, the uncertainty of the pp cross section normalization uncertainty (2.1%) [11] and of the average nuclear overlap function (0.7% for central, 1.6% for mid-central) [45] are included in the global normalization uncertainty.

The systematic uncertainty of the raw-yield extraction was estimated by repeating the invariant mass fits varying the lower and upper limits of the fit range, the functional form of the background fit function, and considering the Gaussian width (mean) as a free (fixed) parameter in the fit. In order to test the sensitivity to the line shape of the signal, a bin-counting method was used, in which the signal yield was obtained by integrating the invariant-mass distribution after subtracting the background estimated from the sideband fit, as well as by studying the signal shape in the MC simulations using multiple stacked Gaussian functions rather than a single one. The procedure to estimate the systematic uncertainty of the track-reconstruction efficiency includes variations of the track-quality selection criteria for all decay tracks and studies on the probability to match TPC tracks to the ITS clusters in data and simulation for the proton-candidate track. The latter comparison was performed after weighting the relative abundances of primary and secondary particles in simulation to those in data [33]. The systematic uncertainty of the Λ_c^+ selection efficiency was estimated by repeating the analysis with different selections on the BDT output, resulting in up to 50% lower and 20–50% higher efficiency values. Possible systematic effects due to the loose PID selection, applied prior to the BDT one, were investigated by comparing the PID-selection efficiencies in data and in simulations and found to be negligible. Both the tracking- and PID-efficiency studies were performed using pure samples of pions (from K_S^0 decays) and protons (from Λ decays). An additional contribution derives from the
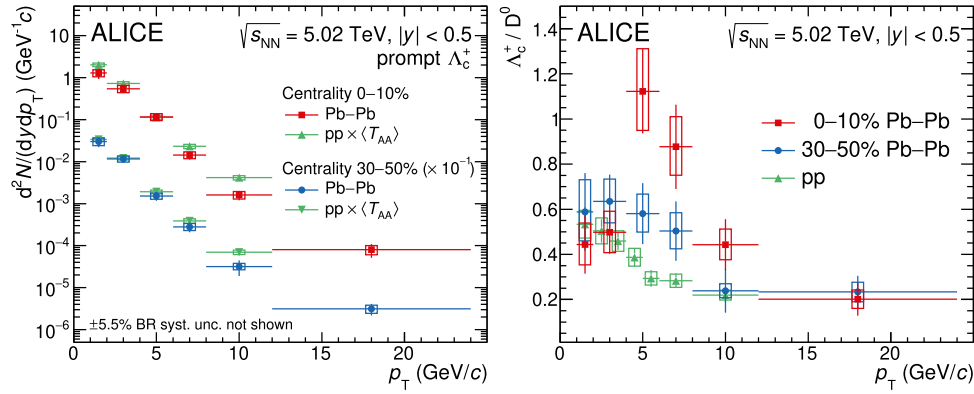
Fig. 1. Left: p_T-differential production yields of prompt Λ_c^+ in central (0–10%) and mid-central (30–50%) Pb–Pb collisions at $\sqrt{s_{NN}} = 5.02$ TeV compared to the pp reference [11] scaled by the $\langle T_{AA} \rangle$ of the corresponding centrality interval [45]. Right: Λ_c^+/D^0 ratio in central and mid-central Pb–Pb collisions at $\sqrt{s_{NN}} = 5.02$ TeV compared with the results obtained from pp collisions [11].

p_T spectra of Λ_c^+ generated in the simulation, which was estimated by using the Λ_c^+/D^0 predictions of the Catania model [7] and the SHMc [10] instead of the TAMU prediction [8] in the p_T-shape reweighting procedure, as well as by an iterative method using a parametrization of the measured p_T-differential production yields. Finally, the systematic uncertainty of the feed-down subtraction was estimated by varying the FONLL parameters as prescribed in [55] and the function describing the Λ_b^0 fragmentation fraction within the quoted experimental uncertainty as reported in [11], as well as by varying the hypothesis on $R_{AA}^{non\text{-}prompt}$. For the latter, an interval $1/3 < R_{AA}^{non\text{-}prompt}/R_{AA}^{prompt} < 3$ was considered, wider with respect to that used for non-strange D mesons [56] to cover possible yet unmeasured differences between the modification of charm- and beauty-baryon production in Pb–Pb collisions with respect to the one in pp collisions.

The sources of systematic uncertainty considered in this analysis are assumed to be uncorrelated among each other and the total systematic uncertainty in each p_T and centrality interval is calculated as the quadratic sum of the individual uncertainties. For the Λ_c^+/D^0 ratio, the Λ_c^+ and D^0 uncertainties were considered as uncorrelated except for the tracking efficiency and the feed-down contribution, which are assumed correlated and thus partially cancel in the ratio, and the systematic uncertainty of the centrality interval definition, which fully cancels. For the R_{AA}, the pp and Pb–Pb uncertainties were considered as uncorrelated except for the branching ratio uncertainty and the feed-down contribution, which both partially cancel out (the former because the pp measurement considers additional decay modes). Finally, in case of the p_T-integrated Λ_c^+/D^0 ratio, there is a correlation between the extrapolation uncertainty of the Λ_c^+ baryon and the measured uncertainties of the Λ_c^+ and D^0 hadrons. To treat this correlation, the extrapolation uncertainty is divided into a correlated part (estimated as the extrapolation uncertainty when considering only the shape predicted by TAMU) and an uncorrelated part (the total extrapolation uncertainty subtracting the correlated part) with respect to the measured uncertainties. The uncorrelated part is summed in quadrature with the measured uncertainties, while the correlated part is added linearly.

4. Results

The p_T-differential production yields of prompt Λ_c^+ baryons are shown in Fig. 1 (left panel). The statistical and total systematic uncertainties are shown as uncertainty bars and boxes, respectively, for all figures. The results are compared with the pp reference cross section [11] multiplied by the corresponding $\langle T_{AA} \rangle$ [45], i.e. the denominator of the R_{AA} observable that is discussed later.

In the right panel of Fig. 1, the ratio of the production yields of Λ_c^+ baryons to that of D^0 mesons, measured in the same centrality intervals [56], are presented together with the pp measurement at the same collision energy [11]. The ratios increase from pp to mid-central and central Pb–Pb collisions for $4 < p_T < 8$ GeV/c with a significance of 2.0 and 3.7 standard deviations, respectively. This trend is qualitatively similar to what is observed for the p/π [58] and Λ/K_S^0 [59] ratios, which both show a distinct peak at intermediate p_T that increases in magnitude (by about a factor 2 for mid-central and a factor 3 for central Pb–Pb collisions with respect to minimum-bias pp collisions) and shifts to higher p_T values (from about 2 GeV/c in pp to 4 GeV/c in central Pb–Pb collisions) with increasing multiplicity. The central and mid-central Λ_c^+/D^0 ratios in $12 < p_T < 24$ GeV/c are compatible with the measurement by CMS in 0–100% Pb–Pb collisions in $p_T > 10$ GeV/c region [15]. The central Λ_c^+/D^0 ratio in $6 < p_T < 8$ GeV/c is in agreement with the previous measurement of ALICE in the 0–80% centrality interval [33]. For $p_T > 4$ GeV/c, the ratio measured in central collisions resembles in magnitude and p_T trend the one reported by STAR in $2.5 < p_T < 8$ GeV/c in 10–80% Au–Au collisions at $\sqrt{s_{NN}} = 200$ GeV [34]. Note that the large centrality classes of the previous measurements are dominated by the production in the most central events (given the scaling of the Λ_c^+ yields with $N_{coll} \times R_{AA}$), hence they are compared to the measurement in 0–10%.

The nuclear modification factor R_{AA} of prompt Λ_c^+ is compared with the R_{AA} of prompt D_s^+ mesons [60] and the average R_{AA} of prompt D^0, D^+, and D^{*+} mesons [56] in Fig. 2 for the 0–10% and 30–50% centrality intervals. The p_T-differential Λ_c^+ cross section in pp collisions at $\sqrt{s} = 5.02$ TeV in the $1 < p_T < 12$ GeV/c interval from [11] was used as the pp reference. In the interval $12 < p_T < 24$ GeV/c, the Λ_c^+ and D^0 measurements at $\sqrt{s} = 5.02$ and 13 TeV [14,61] were exploited, assuming no $\sqrt{s}$ dependence for the Λ_c^+/D^0 ratio as observed within uncertainties in $1 < p_T < 12$ GeV/c [14]. The total uncertainty of the pp reference in the $12 < p_T < 24$ GeV/c interval is 23%, combining in quadrature the measured statistical and systematic uncertainties on the Λ_c^+/D^0 ratio at $\sqrt{s} = 13$ TeV and D^0 cross section at $\sqrt{s} = 5.02$ TeV.

The suppression of all charm-meson (baryon) species from $p_T \gtrsim 3$ (6) GeV/c is understood as being primarily due to the interaction of charm quarks with the quark–gluon plasma, which modifies their momentum spectra, as discussed extensively for the non-strange D mesons in [56]. In central collisions in the region $4 < p_T < 8$ GeV/c, there is a hint of a hierarchy $R_{AA}(D) < R_{AA}(D_s^+) < R_{AA}(\Lambda_c^+)$. In mid-central collisions, this hierarchy is less pronounced. In the $p_T \gtrsim 10$ GeV/c region, where the hadronization is expected to occur mainly via fragmentation, the R_{AA} of the various charm-hadron species are compatible within uncertainties.
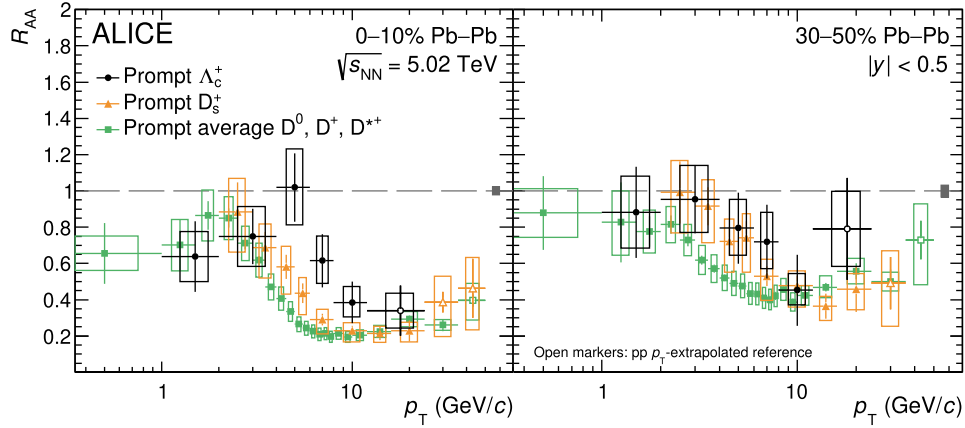
Fig. 2. Nuclear modification factor R_{AA} of prompt Λ_c^+ baryons in central (0–10%; left) and mid-central (30–50%; right) Pb–Pb collisions at $\sqrt{s_{NN}} = 5.02$ TeV, compared with the R_{AA} of prompt D_s^+ [60] and the average of prompt non-strange D mesons [56]. The normalization uncertainties are shown as boxes around unity.
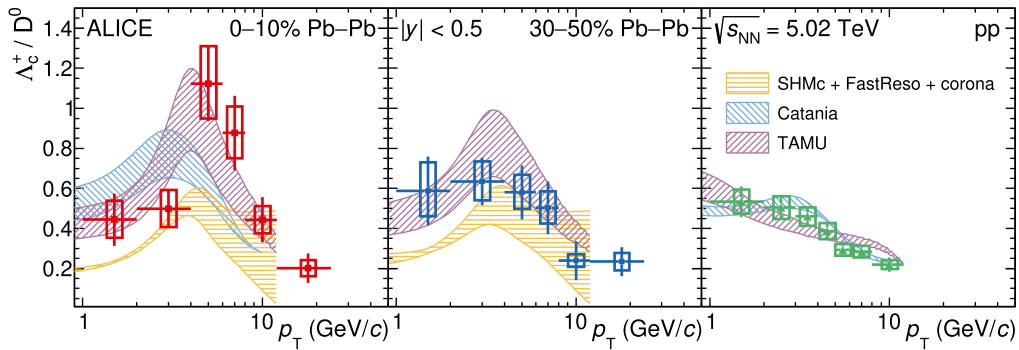

Fig. 3. The Λ_c^+/D^0 yield ratio as a function of p_T in 0–10% (left) and 30–50% (middle) Pb–Pb and pp (right) collisions at $\sqrt{s_{NN}} = 5.02$ TeV compared with predictions of different theoretical calculations [7,8,10,30,31,64].

Fig. 3 compares the p_T-differential Λ_c^+/D^0 ratios with different theoretical predictions: Catania [7], TAMU [8], and the GSI–Heidelberg statistical hadronization model (SHMc) [10]. The predictions of Catania and TAMU for pp collisions [30,31] are also compared with the existing measurement in pp collisions [11]. The Catania model [7,30] assumes that a QGP is formed in both pp and Pb–Pb collisions. In Pb–Pb collisions heavy-quark transport is implemented via the Boltzmann equation, and in both pp and Pb–Pb collisions hadronization occurs either via coalescence, implemented through the Wigner formalism, or via fragmentation in case the quarks do not undergo coalescence. The TAMU model [8] describes charm-quark transport in an expanding medium with the Langevin equation and hadronization proceeds primarily via coalescence, implemented with a Resonance Recombination Model (RRM) [62]. Left-over charm quarks not undergoing coalescence are hadronized via fragmentation. In pp collisions, the charm-hadron abundances are instead determined with a statistical hadronization approach [31]. In both collision systems the underlying charm-baryon spectrum includes unobserved excited states [28] predicted by the Relativistic Quark Model (RQM) [63] and lattice QCD [31]. Finally, for the SHMc predictions [10], which include only charm mesons and baryons established experimentally, the charm-hadron p_T spectra are modeled within a core-corona approach. The core contribution represents the central region of the colliding nuclei where charm quarks achieve local thermal equilibrium in a hydrodynamically expanding QGP. The charm-hadron spectra in the corona contribution are, instead, parameterized from measurements in pp collisions. The p_T-spectra modification due to resonance decays is computed using the FastReso package [64]. The theoretical uncertainty bands shown in

Fig. 3 derive from: an assumed range of branching ratios (50–100%) for the decays of the RQM-augmented excited states into Λ_c^+ for the TAMU model; the variation of about 10% of the Wigner function widths in the Catania calculations; and mainly the uncertainties on the pp spectra fits in the SHMc predictions at high p_T.

The SHMc describes the Λ_c^+/D^0 ratio in mid-central collisions, but underpredicts the ratio in $4 < p_T < 8$ GeV/c in central collisions by about 2.5σ of the combined statistical, systematic, and theoretical uncertainties. The prediction of the Catania model in central collisions underestimates the Λ_c^+/D^0 ratio at intermediate p_T, although the deviation is at maximum 2.5σ. The TAMU predictions reproduce the magnitude and shape of the Λ_c^+/D^0 ratios. While both these fragmentation plus coalescence model calculations are able to describe the Λ_c^+/D^0 ratio in Au–Au collisions at $\sqrt{s_{NN}} = 200$ GeV in the 10–80% centrality interval [34], the TAMU model better reproduces the data in central Pb–Pb collisions. A pure coalescence scenario from an older version of the Catania model was reproducing better the previous ALICE measurement in 0–80% Pb–Pb collisions [33]. The Catania and TAMU predictions also describe both the magnitude and p_T shape of the measured Λ_c^+/D^0 ratio in pp collisions. Instead, at forward rapidity, the TAMU model predicts a systematically higher Λ_c^+/D^0 ratio than measured by LHCb in 65–90% Pb–Pb collisions at $\sqrt{s_{NN}} = 5.02$ TeV [39].

The Λ_c^+ production yield for $p_T > 0$ was estimated by summing up the measured p_T-differential yields and the extrapolated Λ_c^+ yield for $p_T < 1$ GeV/c. The Λ_c^+ yield in $0 < p_T < 1$ GeV/c was obtained as the product of the Λ_c^+/D^0 ratio value estimated by interpolating the ratio in the measured p_T interval
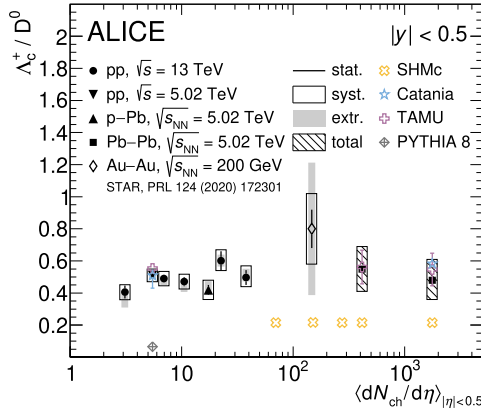
Fig. 4. The p_T-integrated and to $p_T > 0$ extrapolated Λ_c^+/D^0 ratios in central and mid-central Pb–Pb collisions at $\sqrt{s_{NN}} = 5.02$ TeV compared to the same ratio at pp and p–Pb [11,32] and Au–Au [34] multiplicities. Predictions from theoretical calculations are shown as well [7,8,10,23,30,31].

with model expectations and the measured D^0 yield [56]. The interpolation procedure was performed using the shape predicted by TAMU [8], Catania [7] (not available for 30–50%), SHMc [10], and blast-wave [65] calculations, leaving the normalization as a free parameter. The shape from TAMU was chosen as the central value based on the χ^2/ndf values, while the difference between the obtained yields was considered in the systematic uncertainty due to the extrapolation. The results for the prompt Λ_c^+ production yields per unit of rapidity in $|y| < 0.5$ are $dN/dy = 3.27 \pm 0.42\,(\text{stat}) \pm 0.45\,(\text{syst}) \pm 0.16\,(\text{BR})\,^{+0.46}_{-0.29}\,(\text{extr})$ for central collisions and $dN/dy = 0.70 \pm 0.09\,(\text{stat}) \pm 0.09\,(\text{syst}) \pm 0.04\,(\text{BR})\,^{+0.07}_{-0.05}\,(\text{extr})$ for mid-central collisions, where the visible yield is about 81% of the total for both centrality classes. The SHMc [10] predicts lower values, $dN/dy = 1.55 \pm 0.23$ and $dN/dy = 0.316 \pm 0.036$, respectively.

The measured Λ_c^+/D^0 ratios, obtained dividing the p_T-integrated Λ_c^+ and D^0 yields [56], are presented in Fig. 4, taking into account the correlation between the measured and extrapolated uncertainties. Similarly to what is observed for the Λ/K_S^0 ratio [59,66], the Λ_c^+/D^0 ratios in Pb–Pb collisions are compatible with the p_T-integrated Λ_c^+/D^0 ratios at pp and p–Pb multiplicities [11,32] within one standard deviation of the combined uncertainties. This observation, together with the significant enhancement of the Λ_c^+/D^0 ratio at intermediate p_T with increasing multiplicity, seen here and in pp collisions [32], suggests a modified (and perhaps similar) mechanism of hadronization in all hadronic collision systems with respect to charm fragmentation tuned on e^+e^- and e^-p measurements (PYTHIA 8 point in Fig. 4). The coalescence models of [4,5,9], in which the Λ_c^+/D^0 ratio depends on the balance of quark and diquark densities at hadronization time, expect a dependence of the p_T-integrated Λ_c^+/D^0 ratio on multiplicity (leading to an increase by about a factor 3–10 in nuclear collisions compared with their pp baseline), which is not observed. The measured p_T-differential enhancement may, instead, predominantly be caused by altered production ratios for baryons and mesons following from the phase-space distribution of the quarks. This can arise from the collective radial expansion of the system, for which, in the coalescence picture (Catania and TAMU Pb–Pb points in Fig. 4), the accounting of space–momentum correlations in the procedure have been observed to be fundamental in [8,9]. Interactions in the hadronic phase are, on the contrary, expected to have a small effect on the Λ_c^+/D^0 ratio [6,67]. The statistical hadronization approach (SHMc and TAMU pp points in Fig. 4), can also describe both the p_T-differential and p_T-integrated observations with the, currently

debated, caveat that for the proper normalization yet unobserved charm-baryon states need to be assumed [10,31]. Note that the authors of the TAMU model include these additional states already in their predictions, while for the SHMc model it is not the baseline. The uncertainty of the p_T-integrated yield in Pb–Pb collisions is still relatively large, and more precise measurements at low p_T will help to further discriminate between charm-baryon formation scenarios.

Finally, Fig. 5 shows the R_{AA} of prompt Λ_c^+ baryons compared with the previously introduced theoretical models [7,8,10]. The Catania R_{AA} predictions are from an earlier version of the model than the Λ_c^+/D^0 predictions and they do not have an uncertainty band. The TAMU model provides a good description of the R_{AA}, over the whole p_T range, in both central and mid-central collisions. The Catania model describes the data in both central and mid-central collisions for $p_T > 2$ GeV/c, however for $p_T < 2$ GeV/c the model predicts a R_{AA} higher than unity which is disfavored by data. Both these models do not include charm-quark interactions with medium constituents via radiative processes, hence are not expected to describe the R_{AA} for $p_T > 8$ GeV/c. The SHMc model instead significantly underestimates the Λ_c^+ R_{AA} over the whole p_T range.

5. Conclusions

In summary, the measurements of the production yield of prompt Λ_c^+ baryons in central (0–10%) and mid-central (30–50%) Pb–Pb collisions at a center-of-mass energy per nucleon pair $\sqrt{s_{NN}} = 5.02$ TeV were presented. The yield could be extrapolated to $p_T = 0$ in the two centrality classes with significantly smaller uncertainties than the previous measurement by STAR in 10–80% Au–Au collisions at $\sqrt{s_{NN}} = 200$ GeV, exploring not only a new energy regime but also higher multiplicities. The p_T-differential Λ_c^+/D^0 ratios increase from pp to central Pb–Pb collisions for $4 < p_T < 8$ GeV/c with a significance of 3.7 standard deviations, while the p_T-integrated ratios are compatible within one standard deviation. Both observations are in qualitative agreement with the baryon-to-meson ratio for strange hadrons. The measurements are described by theoretical calculations that include both coalescence and fragmentation processes when describing the hadronization of heavy flavors in the QGP. The upgraded ALICE detector for the LHC Runs 3 and 4 will increase its acquisition rate by up to a factor of about 50 in Pb–Pb collisions and the tracking precision by a factor 3–6, meaning future measurements of Λ_c^+-baryon production will allow for stronger constraints on the heavy-quark hadronization mechanisms in heavy-ion collisions [68].

Declaration of competing interest

The authors declare that they have no known competing financial interests or personal relationships that could have appeared to influence the work reported in this paper.

Data availability

Data will be made available on request.
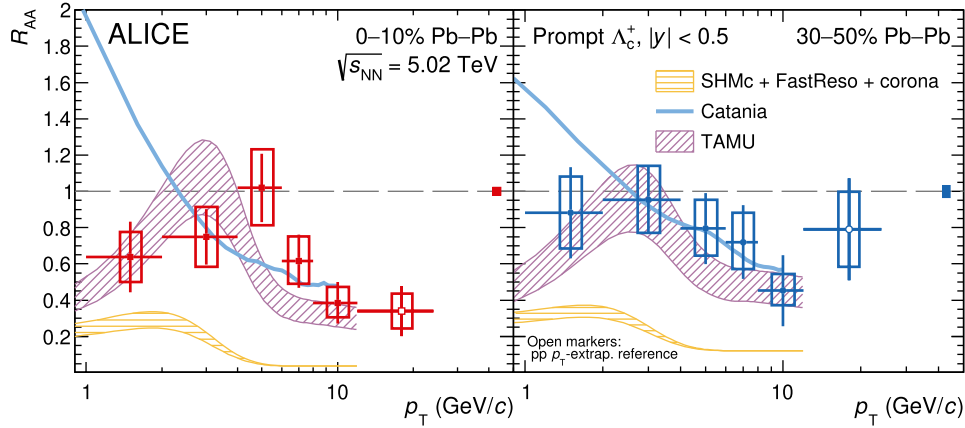
Acknowledgements

Fig. 5. Nuclear modification factor R_{AA} of prompt Λ_c^+ baryons in central (0–10%; left) and mid-central (30–50%; right) Pb–Pb collisions at $\sqrt{s_{NN}} = 5.02$ TeV, compared with model predictions. When estimated, the model uncertainty is shown as a shaded band.

Appendix A. Raw-yield extraction

Examples of the invariant mass distributions from which the Λ_c^+ raw yields are extracted are reported in Fig. A.1. The spectra together with the result of the fits in $1 < p_T < 2$ GeV/c and $4 < p_T < 6$ GeV/c for central (0–10%) and $2 < p_T < 4$ GeV/c and $8 < p_T < 12$ GeV/c for mid-central (30–50%) Pb–Pb collisions are shown.

References

[1] W. Busza, K. Rajagopal, W. van der Schee, Heavy ion collisions: the big picture, and the big questions, Annu. Rev. Nucl. Part. Sci. 68 (2018) 339–376, arXiv:1802.04801 [hep-ph].

[2] B. Muller, J. Schukraft, B. Wyslouch, First results from Pb–Pb collisions at the LHC, Annu. Rev. Nucl. Part. Sci. 62 (2012) 361–386, arXiv:1202.3233 [hep-ex].

[3] A. Andronic, et al., Heavy-flavour and quarkonium production in the LHC era: from proton–proton to heavy-ion collisions, Eur. Phys. J. C 76 (2016) 107, arXiv:1506.03981 [nucl-ex].

[4] S.H. Lee, et al., Λ_c enhancement from strongly coupled quark-gluon plasma, Phys. Rev. Lett. 100 (2008) 222301, arXiv:0709.3637 [nucl-th].

[5] Y. Oh, C.M. Ko, S.H. Lee, S. Yasui, Ratios of heavy baryons to heavy mesons in relativistic nucleus–nucleus collisions, Phys. Rev. C 79 (2009) 044905, arXiv:0901.1382 [nucl-th].

[6] S.K. Das, et al., Propagation of heavy baryons in heavy-ion collisions, Phys. Rev. D 94 (2016) 114039, arXiv:1604.05666 [nucl-th].

[7] S. Plumari, et al., Charmed hadrons from coalescence plus fragmentation in relativistic nucleus–nucleus collisions at RHIC and LHC, Eur. Phys. J. C 78 (2018) 348, arXiv:1712.00730 [hep-ph].
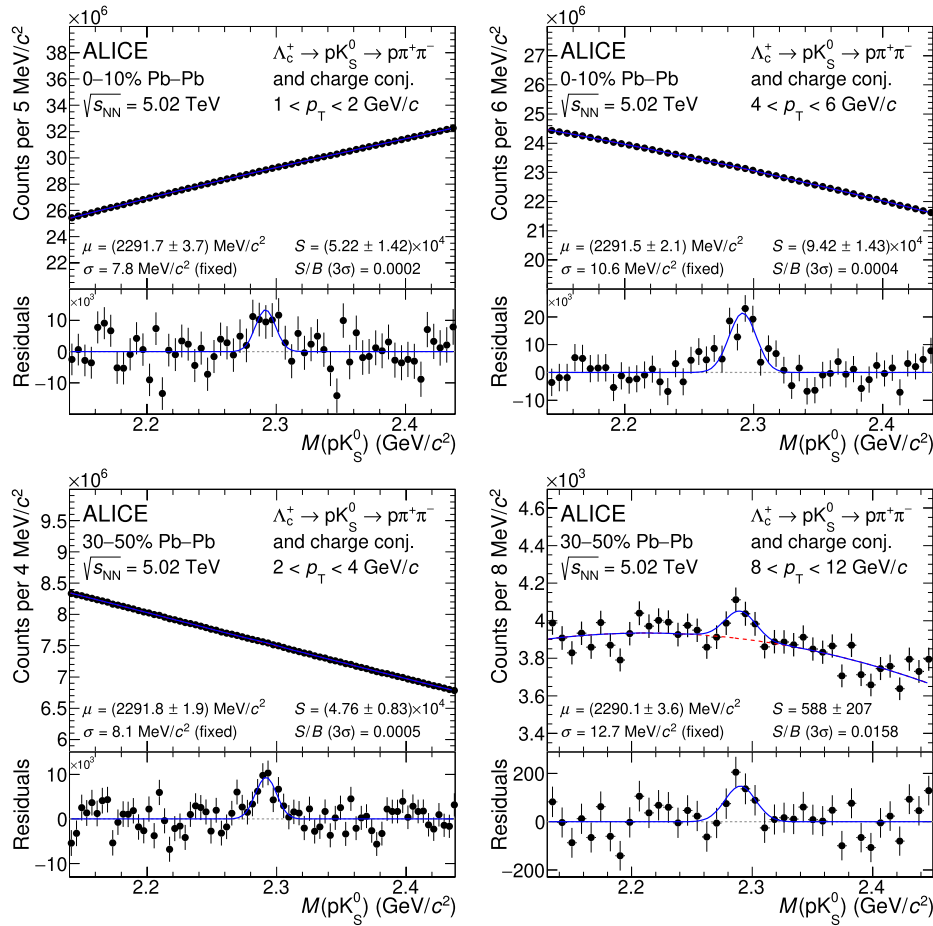
Fig. A.1. Invariant mass (M) distributions of $\Lambda_c^+ \to pK_S^0 \to p\pi^+\pi^-$ candidates and charge conjugates in different p_T intervals in central (0–10%; top) and mid-central (30–50%; bottom) Pb–Pb collisions at $\sqrt{s_{NN}} = 5.02$ TeV. The blue solid lines show the total fit functions and the red dashed lines are the combinatorial-background terms. The values of the mean (μ) and the width (σ) of the signal peak are reported together with the signal counts (S) and the signal-over-background ratio (S/B) in the mass interval ($\mu - 3\sigma, \mu + 3\sigma$).

[8] M. He, R. Rapp, Hadronization and charm-hadron ratios in heavy-ion collisions, Phys. Rev. Lett. 124 (2020) 042301, arXiv:1905.09216 [nucl-th].

[9] A. Beraudo, et al., In-medium hadronization of heavy quarks and its effect on charmed meson and baryon distributions in heavy-ion collisions, arXiv:2202.08732 [hep-ph].

[10] A. Andronic, et al., The multiple-charm hierarchy in the statistical hadronization model, J. High Energy Phys. 07 (2021) 035, arXiv:2104.12754 [hep-ph].

[11] ALICE Collaboration, S. Acharya, et al., Λ_c^+ production in pp and in p–Pb collisions at $\sqrt{s_{NN}} = 5.02$ TeV, Phys. Rev. C 104 (2021) 054905, arXiv:2011.06079 [nucl-ex].

[12] ALICE Collaboration, S. Acharya, et al., Λ_c^+ production and baryon-to-meson ratios in pp and p–Pb collisions at $\sqrt{s_{NN}} = 5.02$ TeV at the LHC, Phys. Rev. Lett. 127 (2021) 202301, arXiv:2011.06078 [nucl-ex].

[13] ALICE Collaboration, S. Acharya, et al., Λ_c^+ production in pp collisions at $\sqrt{s} = 7$ TeV and in p–Pb collisions at $\sqrt{s_{NN}} = 5.02$ TeV, J. High Energy Phys. 04 (2018) 108, arXiv:1712.09581 [nucl-ex].

[14] ALICE Collaboration, S. Acharya, et al., Measurement of prompt D^0, Λ_c^+, and $\Sigma_c^{0,++}(2455)$ production in pp collisions at $\sqrt{s} = 13$ TeV, Phys. Rev. Lett. 128 (2022) 012001, arXiv:2106.08278 [hep-ex].

[15] CMS Collaboration, A.M. Sirunyan, et al., Production of Λ_c^+ baryons in proton–proton and lead–lead collisions at $\sqrt{s_{NN}} = 5.02$ TeV, Phys. Lett. B 803 (2020) 135328, arXiv:1906.03322 [hep-ex].

[16] LHCb Collaboration, R. Aaij, et al., Prompt charm production in pp collisions at $\sqrt{s} = 7$ TeV, Nucl. Phys. B 871 (2013) 1–20, arXiv:1302.2864 [hep-ex].

[17] ARGUS Collaboration, H. Albrecht, et al., Observation of the charmed baryon Λ_c in e^+e^- annihilation at 10 GeV, Phys. Lett. B 207 (1988) 109–114.

[18] CLEO Collaboration, P. Avery, et al., Inclusive production of the charmed baryon Λ_c^+ from e^+e^- annihilations at $\sqrt{s} = 10.55$ GeV, Phys. Rev. D 43 (1991) 3599–3610.

[19] ARGUS Collaboration, H. Albrecht, et al., Inclusive production of D^0, D^+ and $D^{*+}(2010)$ mesons in B decays and nonresonant e^+e^- annihilation at 10.6 GeV, Z. Phys. C 52 (1991) 353–360.

[20] ZEUS Collaboration, S. Chekanov, et al., Measurement of charm fragmentation ratios and fractions in photoproduction at HERA, Eur. Phys. J. C 44 (2005) 351–366, arXiv:hep-ex/0508019.

[21] ZEUS Collaboration, H. Abramowicz, et al., Measurement of charm fragmentation fractions in photoproduction at HERA, J. High Energy Phys. 09 (2013) 058, arXiv:1306.4862 [hep-ex].

[22] ZEUS Collaboration, H. Abramowicz, et al., Measurement of D^+ and Λ_c^+ production in deep inelastic scattering at HERA, J. High Energy Phys. 11 (2010) 009, arXiv:1007.1945 [hep-ex].

[23] T. Sjöstrand, et al., An introduction to PYTHIA 8.2, Comput. Phys. Commun. 191 (2015) 159–177, arXiv:1410.3012 [hep-ph].

[24] M. Bahr, et al., Herwig++ physics and manual, Eur. Phys. J. C 58 (2008) 639–707, arXiv:0803.0883 [hep-ph].

[25] S. Frixione, P. Nason, G. Ridolfi, A positive-weight next-to-leading-order Monte Carlo for heavy flavour hadroproduction, J. High Energy Phys. 09 (2007) 126, arXiv:0707.3088 [hep-ph].

[26] B.A. Kniehl, G. Kramer, I. Schienbein, H. Spiesberger, $\Lambda_c^\pm$ production in pp collisions with a new fragmentation function, Phys. Rev. D 101 (2020) 114021, arXiv:2004.04213 [hep-ph].

[27] L. Gladilin, Fragmentation fractions of c and b quarks into charmed hadrons at LEP, Eur. Phys. J. C 75 (2015) 19, arXiv:1404.3888 [hep-ex].

[28] Particle Data Group Collaboration, P. Zyla, et al., Review of particle physics, PTEP 2020 (2020), 083C01.

[29] J.R. Christiansen, P.Z. Skands, String formation beyond leading colour, J. High Energy Phys. 08 (2015) 003, arXiv:1505.01681 [hep-ph].

[30] V. Minissale, S. Plumari, V. Greco, Charm hadrons in pp collisions at LHC energy within a coalescence plus fragmentation approach, Phys. Lett. B 821 (2021) 136622, arXiv:2012.12001 [hep-ph].

[31] M. He, R. Rapp, Charm-baryon production in proton–proton collisions, Phys. Lett. B 795 (2019) 117–121, arXiv:1902.08889 [nucl-th].

[32] ALICE Collaboration, S. Acharya, et al., Observation of a multiplicity dependence in the p_T-differential charm baryon-to-meson ratios in proton–proton collisions at $\sqrt{s} = 13$ TeV, Phys. Lett. B 829 (2022) 137065, arXiv:2111.11948 [nucl-ex].

[33] ALICE Collaboration, S. Acharya, et al., Λ_c^+ production in Pb–Pb collisions at $\sqrt{s_{NN}} = 5.02$ TeV, Phys. Lett. B 793 (2019) 212–223, arXiv:1809.10922 [nucl-ex].

[34] STAR Collaboration, J. Adam, et al., First measurement of Λ_c baryon production in Au + Au collisions at $\sqrt{s_{NN}} = 200$ GeV, Phys. Rev. Lett. 124 (2020) 172301, arXiv:1910.14628 [nucl-ex].

[35] S. Cho, et al., Charmed hadron production in an improved quark coalescence model, Phys. Rev. C 101 (2020) 024909, arXiv:1905.09774 [nucl-th].

[36] J. Zhao, S. Shi, N. Xu, P. Zhuang, Sequential coalescence with charm conservation in high energy nuclear collisions, arXiv:1805.10858 [hep-ph].

[37] S. Cao, et al., Charmed hadron chemistry in relativistic heavy-ion collisions, Phys. Lett. B 807 (2020) 135561, arXiv:1911.00456 [nucl-th].

[38] LHCb Collaboration, R. Aaij, et al., Prompt Λ_c^+ production in p–Pb collisions at $\sqrt{s_{NN}} = 5.02$ TeV, J. High Energy Phys. 02 (2019) 102, arXiv:1809.01404 [hep-ex].

[39] LHCb Collaboration, R. Aaij, et al., Measurement of the Λ_c^+ to D^0 production cross-section ratio in peripheral Pb–Pb collisions, arXiv:2210.06939 [hep-ex].

[40] ALICE Collaboration, K. Aamodt, et al., The ALICE experiment at the CERN LHC, J. Instrum. 3 (2008) S08002.

[41] ALICE Collaboration, B. Abelev, et al., Performance of the ALICE experiment at the CERN LHC, Int. J. Mod. Phys. A 29 (2014) 1430044, arXiv:1402.4476 [nucl-ex].

[42] ALICE Collaboration, E. Abbas, et al., Performance of the ALICE VZERO system, J. Instrum. 8 (2013) P10016, arXiv:1306.3130 [nucl-ex].

[43] R. Arnaldi, et al., The zero degree calorimeters for the ALICE experiment, Nucl. Instrum. Methods A 581 (2007) 397–401, Erratum: Nucl. Instrum. Methods A 604 (2009) 765.

[44] ALICE Collaboration, S. Acharya, et al., Measurement of D^0, D^+, D^{*+} and D_s^+ production in Pb–Pb collisions at $\sqrt{s_{NN}} = 5.02$ TeV, J. High Energy Phys. 10 (2018) 174, arXiv:1804.09083 [nucl-ex].

[45] ALICE Collaboration, S. Acharya, et al., Centrality determination in heavy ion collisions, ALICE-PUBLIC-2018-011, https://cds.cern.ch/record/2636623.

[46] X.-N. Wang, M. Gyulassy, HIJING: a Monte Carlo model for multiple jet production in pp, pA, and AA collisions, Phys. Rev. D 44 (1991) 3501–3516.

[47] P. Skands, S. Carrazza, J. Rojo, Tuning PYTHIA 8.1: the monash 2013 tune, Eur. Phys. J. C 74 (2014) 3024, arXiv:1404.5630 [hep-ph].

[48] R. Brun, et al., GEANT: detector description and simulation tool, CERN-W-5013, http://cds.cern.ch/record/1082634.

[49] ALICE Collaboration, K. Aamodt, et al., Alignment of the ALICE inner tracking system with cosmic-ray tracks, J. Instrum. 5 (2010) P03003, arXiv:1001.0502 [physics.ins-det].

[50] J. Alme, et al., The ALICE TPC, a large 3-dimensional tracking device with fast readout for ultra-high multiplicity events, Nucl. Instrum. Methods A 622 (2010) 316–367, arXiv:1001.1950 [physics.ins-det].

[51] T. Chen, C. Guestrin, XGBoost: a scalable tree boosting system, in: Proceedings of the 22nd ACM SIGKDD International Conference on Knowledge Discovery and Data Mining, 2016, pp. 785–794, arXiv:1603.02754 [cs.LG].

[52] A. Akindinov, et al., Performance of the ALICE time-of-flight detector at the LHC, Eur. Phys. J. Plus 128 (2013) 44.

[53] ALICE Collaboration, J. Adam, et al., Determination of the event collision time with the ALICE detector at the LHC, Eur. Phys. J. Plus 132 (2017) 99, arXiv:1610.03055 [physics.ins-det].

[54] M. Cacciari, M. Greco, P. Nason, The p_T spectrum in heavy-flavour hadroproduction, J. High Energy Phys. 05 (1998) 007, arXiv:hep-ph/9803400 [hep-ph].

[55] M. Cacciari, et al., Theoretical predictions for charm and bottom production at the LHC, J. High Energy Phys. 10 (2012) 137, arXiv:1205.6344 [hep-ph].

[56] ALICE Collaboration, S. Acharya, et al., Prompt D^0, D^+ and D^{*+} production in Pb–Pb collisions at $\sqrt{s_{NN}} = 5.02$ TeV, J. High Energy Phys. 01 (2022) 174, arXiv:2110.09420 [nucl-ex].

[57] LHCb Collaboration, R. Aaij, et al., Measurement of b hadron fractions in 13 TeV pp collisions, Phys. Rev. D 100 (2019) 031102, arXiv:1902.06794 [hep-ex].

[58] ALICE Collaboration, S. Acharya, et al., Production of charged pions, kaons, and (anti-)protons in Pb–Pb and inelastic pp collisions at $\sqrt{s_{NN}} = 5.02$ TeV, Phys. Rev. C 101 (2020) 044907, arXiv:1910.07678 [nucl-ex].

[59] ALICE Collaboration, B. Abelev, et al., K_S^0 and Λ production in Pb–Pb collisions at $\sqrt{s_{NN}} = 2.76$ TeV, Phys. Rev. Lett. 111 (2013) 222301, arXiv:1307.5530 [nucl-ex].

[60] ALICE Collaboration, S. Acharya, et al., Measurement of prompt D_s^+-meson production and azimuthal anisotropy in Pb–Pb collisions at $\sqrt{s_{NN}} = 5.02$ TeV, Phys. Lett. B 827 (2022) 136986, arXiv:2110.10006 [nucl-ex].

[61] ALICE Collaboration, S. Acharya, et al., Measurement of D^0, D^+, D^{*+} and D_s^+ production in pp collisions at $\sqrt{s} = 5.02$ TeV with ALICE, Eur. Phys. J. C 79 (2019) 388, arXiv:1901.07979 [nucl-ex].

[62] L. Ravagli, R. Rapp, Quark coalescence based on a transport equation, Phys. Lett. B 655 (2007) 126–131, arXiv:0705.0021 [hep-ph].

[63] D. Ebert, R.N. Faustov, V.O. Galkin, Spectroscopy and Regge trajectories of heavy baryons in the relativistic quark-diquark picture, Phys. Rev. D 84 (2011) 014025, arXiv:1105.0583 [hep-ph].

[64] A. Mazeliauskas, S. Floerchinger, E. Grossi, D. Teaney, Fast resonance decays in nuclear collisions, Eur. Phys. J. C 79 (2019) 284, arXiv:1809.11049 [nucl-th].

[65] E. Schnedermann, J. Sollfrank, U.W. Heinz, Thermal phenomenology of hadrons from 200A GeV S+S collisions, Phys. Rev. C 48 (1993) 2462–2475, arXiv:nucl-th/9307020.

[66] ALICE Collaboration, S. Acharya, et al., Multiplicity dependence of (multi-)strange hadron production in proton–proton collisions at $\sqrt{s} = 13$ TeV, Eur. Phys. J. C 80 (2020) 167, arXiv:1908.01861 [nucl-ex].

[67] S. Ghosh, et al., Diffusion of Λ_c in hot hadronic medium and its impact on Λ_c/D ratio, Phys. Rev. D 90 (2014) 054018, arXiv:1407.5069 [nucl-th].

[68] Z. Citron, et al., Report from working group 5: future physics opportunities for high-density QCD at the LHC with heavy-ion and proton beams, CERN Yellow Rep. Monogr. 7 (2019) 1159–1410, arXiv:1812.06772 [hep-ph].

ALICE Collaboration

S. Acharya [142], D. Adamová [96], A. Adler [74], J. Adolfsson [81], G. Aglieri Rinella [34], M. Agnello [30], N. Agrawal [54], Z. Ahammed [142], S. Ahmad [16], S.U. Ahn [76], I. Ahuja [38], Z. Akbar [51], A. Akindinov [93], M. Al-Turany [108], S.N. Alam [16], D. Aleksandrov [89], B. Alessandro [59], H.M. Alfanda [7], R. Alfaro Molina [71], B. Ali [16], Y. Ali [14], A. Alici [25], N. Alizadehvandchali [125], A. Alkin [34], J. Alme [21], G. Alocco [55], T. Alt [68], I. Altsybeev [113], M.N. Anaam [7], C. Andrei [48], D. Andreou [91], A. Andronic [145], V. Anguelov [105], F. Antinori [57], P. Antonioli [54], C. Anuj [16], N. Apadula [80], L. Aphecetche [115], H. Appelshäuser [68], S. Arcelli [25], R. Arnaldi [59], I.C. Arsene [20], M. Arslandok [147], A. Augustinus [34], R. Averbeck [108], S. Aziz [78], M.D. Azmi [16], A. Badalà [56], Y.W. Baek [41], X. Bai [129,108], R. Bailhache [68], Y. Bailung [50], R. Bala [102], A. Balbino [30], A. Baldisseri [139], B. Balis [2], D. Banerjee [4], Z. Banoo [102], R. Barbera [26], L. Barioglio [106], M. Barlou [85], G.G. Barnaföldi [146], L.S. Barnby [95], V. Barret [136], C. Bartels [128], K. Barth [34], E. Bartsch [68], F. Baruffaldi [27], N. Bastid [136], S. Basu [81], G. Batigne [115], B. Batyunya [75], D. Bauri [49], J.L. Bazo Alba [112], I.G. Bearden [90], C. Beattie [147], P. Becht [108], I. Belikov [138], A.D.C. Bell Hechavarria [145], F. Bellini [25], R. Bellwied [125], S. Belokurova [113], V. Belyaev [94], G. Bencedi [146,69], S. Beole [24], A. Bercuci [48], Y. Berdnikov [99], A. Berdnikova [105], L. Bergmann [105], M.G. Besoiu [67], L. Betev [34], P.P. Bhaduri [142], A. Bhasin [102], I.R. Bhat [102], M.A. Bhat [4], B. Bhattacharjee [42], P. Bhattacharya [22], L. Bianchi [24], N. Bianchi [52], J. Bielčík [37], J. Bielčíková [96], J. Biernat [118], A. Bilandzic [106], G. Biro [146], S. Biswas [4], J.T. Blair [119], D. Blau [89,82], M.B. Blidaru [108], C. Blume [68], G. Boca [28,58], F. Bock [97], A. Bogdanov [94], S. Boi [22], J. Bok [61], L. Boldizsár [146], A. Bolozdynya [94], M. Bombara [38], P.M. Bond [34], G. Bonomi [141,58], H. Borel [139], A. Borissov [82], H. Bossi [147], E. Botta [24], L. Bratrud [68], P. Braun-Munzinger [108], M. Bregant [121], M. Broz [37], G.E. Bruno [107,33], M.D. Buckland [23,128], D. Budnikov [109], H. Buesching [68], S. Bufalino [30], O. Bugnon [115], P. Buhler [114], Z. Buthelezi [72,132], J.B. Butt [14],

A. Bylinkin [127], S.A. Bysiak [118], M. Cai [27,7], H. Caines [147], A. Caliva [108], E. Calvo Villar [112], J.M.M. Camacho [120], R.S. Camacho [45], P. Camerini [23], F.D.M. Canedo [121], M. Carabas [135], F. Carnesecchi [34,25], R. Caron [137,139], J. Castillo Castellanos [139], E.A.R. Casula [22], F. Catalano [30], C. Ceballos Sanchez [75], I. Chakaberia [80], P. Chakraborty [49], S. Chandra [142], S. Chapeland [34], M. Chartier [128], S. Chattopadhyay [142], S. Chattopadhyay [110], T.G. Chavez [45], T. Cheng [7], C. Cheshkov [137], B. Cheynis [137], V. Chibante Barroso [34], D.D. Chinellato [122], S. Cho [61], P. Chochula [34], P. Christakoglou [91], C.H. Christensen [90], P. Christiansen [81], T. Chujo [134], C. Cicalo [55], L. Cifarelli [25], F. Cindolo [54], M.R. Ciupek [108], G. Clai [54,II], J. Cleymans [124,I], F. Colamaria [53], J.S. Colburn [111], D. Colella [53,107,33], A. Collu [80], M. Colocci [34], M. Concas [59,III], G. Conesa Balbastre [79], Z. Conesa del Valle [78], G. Contin [23], J.G. Contreras [37], M.L. Coquet [139], T.M. Cormier [97], P. Cortese [31], M.R. Cosentino [123], F. Costa [34], S. Costanza [28,58], P. Crochet [136], R. Cruz-Torres [80], E. Cuautle [69], P. Cui [7], L. Cunqueiro [97], A. Dainese [57], M.C. Danisch [105], A. Danu [67], P. Das [87], P. Das [4], S. Das [4], S. Dash [49], A. De Caro [29], G. de Cataldo [53], L. De Cilladi [24], J. de Cuveland [39], A. De Falco [22], D. De Gruttola [29], N. De Marco [59], C. De Martin [23], S. De Pasquale [29], S. Deb [50], H.F. Degenhardt [121], K.R. Deja [143], R. Del Grande [106], L. Dello Stritto [29], W. Deng [7], P. Dhankher [19], D. Di Bari [33], A. Di Mauro [34], R.A. Diaz [8], T. Dietel [124], Y. Ding [137,7], R. Divià [34], D.U. Dixit [19], Ø. Djuvsland [21], U. Dmitrieva [63], J. Do [61], A. Dobrin [67], B. Dönigus [68], A.K. Dubey [142], A. Dubla [108,91], S. Dudi [101], P. Dupieux [136], M. Durkac [117], N. Dzalaiova [13], T.M. Eder [145], R.J. Ehlers [97], V.N. Eikeland [21], F. Eisenhut [68], D. Elia [53], B. Erazmus [115], F. Ercolessi [25], F. Erhardt [100], A. Erokhin [113], M.R. Ersdal [21], B. Espagnon [78], G. Eulisse [34], D. Evans [111], S. Evdokimov [92], L. Fabbietti [106], M. Faggin [27], J. Faivre [79], F. Fan [7], W. Fan [80], A. Fantoni [52], M. Fasel [97], P. Fecchio [30], A. Feliciello [59], G. Feofilov [113], A. Fernández Téllez [45], A. Ferrero [139], A. Ferretti [24], V.J.G. Feuillard [105], J. Figiel [118], V. Filova [37], D. Finogeev [63], F.M. Fionda [55], G. Fiorenza [34], F. Flor [125], A.N. Flores [119], S. Foertsch [72], S. Fokin [89], E. Fragiacomo [60], E. Frajna [146], A. Francisco [136], U. Fuchs [34], N. Funicello [29], C. Furget [79], A. Furs [63], J.J. Gaardhøje [90], M. Gagliardi [24], A.M. Gago [112], A. Gal [138], C.D. Galvan [120], P. Ganoti [85], C. Garabatos [108], J.R.A. Garcia [45], E. Garcia-Solis [10], K. Garg [115], C. Gargiulo [34], A. Garibli [88], K. Garner [145], P. Gasik [108], E.F. Gauger [119], A. Gautam [127], M.B. Gay Ducati [70], M. Germain [115], P. Ghosh [142], S.K. Ghosh [4], M. Giacalone [25], P. Gianotti [52], P. Giubellino [108,59], P. Giubilato [27], A.M.C. Glaenzer [139], P. Glässel [105], E. Glimos [131], D.J.Q. Goh [83], V. Gonzalez [144], L.H. González-Trueba [71], S. Gorbunov [39], M. Gorgon [2], L. Görlich [118], S. Gotovac [35], V. Grabski [71], L.K. Graczykowski [143], L. Greiner [80], A. Grelli [62], C. Grigoras [34], V. Grigoriev [94], S. Grigoryan [75,1], F. Grosa [34,59], J.F. Grosse-Oetringhaus [34], R. Grosso [108], D. Grund [37], G.G. Guardiano [122], R. Guernane [79], M. Guilbaud [115], K. Gulbrandsen [90], T. Gunji [133], W. Guo [7], A. Gupta [102], R. Gupta [102], S.P. Guzman [45], L. Gyulai [146], M.K. Habib [108], C. Hadjidakis [78], H. Hamagaki [83], M. Hamid [7], R. Hannigan [119], M.R. Haque [143], A. Harlenderova [108], J.W. Harris [147], A. Harton [10], J.A. Hasenbichler [34], H. Hassan [97], D. Hatzifotiadou [54], P. Hauer [43], L.B. Havener [147], S.T. Heckel [106], E. Hellbär [108], H. Helstrup [36], T. Herman [37], E.G. Hernandez [45], G. Herrera Corral [9], F. Herrmann [145], K.F. Hetland [36], H. Hillemanns [34], C. Hills [128], B. Hippolyte [138], B. Hofman [62], B. Hohlweger [91], J. Honermann [145], G.H. Hong [148], D. Horak [37], S. Hornung [108], A. Horzyk [2], R. Hosokawa [15], Y. Hou [7], P. Hristov [34], C. Hughes [131], P. Huhn [68], L.M. Huhta [126], C.V. Hulse [78], T.J. Humanic [98], H. Hushnud [110], L.A. Husova [145], A. Hutson [125], J.P. Iddon [34,128], R. Ilkaev [109], H. Ilyas [14], M. Inaba [134], G.M. Innocenti [34], M. Ippolitov [89], A. Isakov [96], T. Isidori [127], M.S. Islam [110], M. Ivanov [108], V. Ivanov [99], V. Izucheev [92], M. Jablonski [2], B. Jacak [80], N. Jacazio [34], P.M. Jacobs [80], S. Jadlovska [117], J. Jadlovsky [117], S. Jaelani [62], C. Jahnke [122,121], M.J. Jakubowska [143], A. Jalotra [102], M.A. Janik [143], T. Janson [74], M. Jercic [100], O. Jevons [111], A.A.P. Jimenez [69], F. Jonas [97,145], P.G. Jones [111], J.M. Jowett [34,108], J. Jung [68], M. Jung [68], A. Junique [34], A. Jusko [111], M.J. Kabus [143], J. Kaewjai [116], P. Kalinak [64], A.S. Kalteyer [108], A. Kalweit [34], V. Kaplin [94], A. Karasu Uysal [77], D. Karatovic [100], O. Karavichev [63], T. Karavicheva [63], P. Karczmarczyk [143], E. Karpechev [63], V. Kashyap [87], A. Kazantsev [89], U. Kebschull [74], R. Keidel [47], D.L.D. Keijdener [62], M. Keil [34], B. Ketzer [43], A.M. Khan [7], S. Khan [16], A. Khanzadeev [99], Y. Kharlov [92,82], A. Khatun [16], A. Khuntia [118], B. Kileng [36], B. Kim [17,61], C. Kim [17], D.J. Kim [126], E.J. Kim [73], J. Kim [148], J.S. Kim [41], J. Kim [105], J. Kim [73], M. Kim [105], S. Kim [18], T. Kim [148], S. Kirsch [68], I. Kisel [39], S. Kiselev [93], A. Kisiel [143], J.P. Kitowski [2], J.L. Klay [6], J. Klein [34], S. Klein [80], C. Klein-Bösing [145], M. Kleiner [68], T. Klemenz [106], A. Kluge [34], A.G. Knospe [125], C. Kobdaj [116], T. Kollegger [108], A. Kondratyev [75], N. Kondratyeva [94], E. Kondratyuk [92], J. Konig [68], S.A. Konigstorfer [106], P.J. Konopka [34], G. Kornakov [143], S.D. Koryciak [2], A. Kotliarov [96], O. Kovalenko [86], V. Kovalenko [113], M. Kowalski [118], I. Králik [64], A. Kravčáková [38], L. Kreis [108],

M. Krivda [111,64], F. Krizek [96], K. Krizkova Gajdosova [37], M. Kroesen [105], M. Krüger [68], D.M. Krupova [37],
E. Kryshen [99], M. Krzewicki [39], V. Kučera [34], C. Kuhn [138], P.G. Kuijer [91], T. Kumaoka [134], D. Kumar [142],
L. Kumar [101], N. Kumar [101], S. Kundu [34], P. Kurashvili [86], A. Kurepin [63], A.B. Kurepin [63], A. Kuryakin [109],
S. Kushpil [96], J. Kvapil [111], M.J. Kweon [61], J.Y. Kwon [61], Y. Kwon [148], S.L. La Pointe [39], P. La Rocca [26],
Y.S. Lai [80], A. Lakrathok [116], M. Lamanna [34], R. Langoy [130], P. Larionov [34,52], E. Laudi [34], L. Lautner [34,106],
R. Lavicka [114,37], T. Lazareva [113], R. Lea [141,23,58], J. Lehrbach [39], R.C. Lemmon [95], I. León Monzón [120],
E.D. Lesser [19], M. Lettrich [34,106], P. Lévai [146], X. Li [11], X.L. Li [7], J. Lien [130], R. Lietava [111], B. Lim [17],
S.H. Lim [17], V. Lindenstruth [39], A. Lindner [48], C. Lippmann [108], A. Liu [19], D.H. Liu [7], J. Liu [128], I.M. Lofnes [21],
V. Loginov [94], C. Loizides [97], P. Loncar [35], J.A. Lopez [105], X. Lopez [136], E. López Torres [8], J.R. Luhder [145],
M. Lunardon [27], G. Luparello [60], Y.G. Ma [40], A. Maevskaya [63], M. Mager [34], T. Mahmoud [43], A. Maire [138],
M. Malaev [99], N.M. Malik [102], Q.W. Malik [20], S.K. Malik [102], L. Malinina [75,IV], D. Mal'Kevich [93],
D. Mallick [87], N. Mallick [50], G. Mandaglio [32,56], V. Manko [89], F. Manso [136], V. Manzari [53], Y. Mao [7],
G.V. Margagliotti [23], A. Margotti [54], A. Marín [108], C. Markert [119], M. Marquard [68], N.A. Martin [105],
P. Martinengo [34], J.L. Martinez [125], M.I. Martínez [45], G. Martínez García [115], S. Masciocchi [108],
M. Masera [24], A. Masoni [55], L. Massacrier [78], A. Mastroserio [140,53], A.M. Mathis [106], O. Matonoha [81],
P.F.T. Matuoka [121], A. Matyja [118], C. Mayer [118], A.L. Mazuecos [34], F. Mazzaschi [24], M. Mazzilli [34],
J.E. Mdhluli [132], A.F. Mechler [68], Y. Melikyan [63], A. Menchaca-Rocha [71], E. Meninno [114,29], A.S. Menon [125],
M. Meres [13], S. Mhlanga [124,72], Y. Miake [134], L. Micheletti [59], L.C. Migliorin [137], D.L. Mihaylov [106],
K. Mikhaylov [75,93], A.N. Mishra [146], D. Miśkowiec [108], A. Modak [4], A.P. Mohanty [62], B. Mohanty [87],
M. Mohisin Khan [16,V], M.A. Molander [44], Z. Moravcova [90], C. Mordasini [106], D.A. Moreira De Godoy [145],
I. Morozov [63], A. Morsch [34], T. Mrnjavac [34], V. Muccifora [52], E. Mudnic [35], D. Mühlheim [145], S. Muhuri [142],
J.D. Mulligan [80], A. Mulliri [22], M.G. Munhoz [121], R.H. Munzer [68], H. Murakami [133], S. Murray [124],
L. Musa [34], J. Musinsky [64], J.W. Myrcha [143], B. Naik [132], R. Nair [86], B.K. Nandi [49], R. Nania [54], E. Nappi [53],
A.F. Nassirpour [81], A. Nath [105], C. Nattrass [131], A. Neagu [20], A. Negru [135], L. Nellen [69], S.V. Nesbo [36],
G. Neskovic [39], D. Nesterov [113], B.S. Nielsen [90], E.G. Nielsen [90], S. Nikolaev [89], S. Nikulin [89], V. Nikulin [99],
F. Noferini [54], S. Noh [12], P. Nomokonov [75], J. Norman [128], N. Novitzky [134], P. Nowakowski [143], A. Nyanin [89],
J. Nystrand [21], M. Ogino [83], A. Ohlson [81], V.A. Okorokov [94], J. Oleniacz [143], A.C. Oliveira Da Silva [131],
M.H. Oliver [147], A. Onnerstad [126], C. Oppedisano [59], A. Ortiz Velasquez [69], T. Osako [46], A. Oskarsson [81],
J. Otwinowski [118], M. Oya [46], K. Oyama [83], Y. Pachmayer [105], S. Padhan [49], D. Pagano [141,58], G. Paić [69],
A. Palasciano [53], J. Pan [144], S. Panebianco [139], J. Park [61], J.E. Parkkila [126], S.P. Pathak [125], R.N. Patra [102,34],
B. Paul [22], H. Pei [7], T. Peitzmann [62], X. Peng [7], L.G. Pereira [70], H. Pereira Da Costa [139], D. Peresunko [89,82],
G.M. Perez [8], S. Perrin [139], Y. Pestov [5], V. Petráček [37], M. Petrovici [48], R.P. Pezzi [115,70], S. Piano [60],
M. Pikna [13], P. Pillot [115], O. Pinazza [54,34], L. Pinsky [125], C. Pinto [26], S. Pisano [52], M. Płoskoń [80],
M. Planinic [100], F. Pliquett [68], M.G. Poghosyan [97], B. Polichtchouk [92], S. Politano [30], N. Poljak [100], A. Pop [48],
S. Porteboeuf-Houssais [136], J. Porter [80], V. Pozdniakov [75], S.K. Prasad [4], R. Preghenella [54], F. Prino [59],
C.A. Pruneau [144], I. Pshenichnov [63], M. Puccio [34], S. Qiu [91], L. Quaglia [24], R.E. Quishpe [125], S. Ragoni [111],
A. Rakotozafindrabe [139], L. Ramello [31], F. Rami [138], S.A.R. Ramirez [45], A.G.T. Ramos [33], T.A. Rancien [79],
R. Raniwala [103], S. Raniwala [103], S.S. Räsänen [44], R. Rath [50], I. Ravasenga [91], K.F. Read [97,131],
A.R. Redelbach [39], K. Redlich [86,VI], A. Rehman [21], P. Reichelt [68], F. Reidt [34], H.A. Reme-ness [36],
Z. Rescakova [38], K. Reygers [105], A. Riabov [99], V. Riabov [99], T. Richert [81], M. Richter [20], W. Riegler [34],
F. Riggi [26], C. Ristea [67], M. Rodríguez Cahuantzi [45], K. Røed [20], R. Rogalev [92], E. Rogochaya [75],
T.S. Rogoschinski [68], D. Rohr [34], D. Röhrich [21], P.F. Rojas [45], S. Rojas Torres [37], P.S. Rokita [143],
F. Ronchetti [52], A. Rosano [32,56], E.D. Rosas [69], A. Rossi [57], A. Roy [50], P. Roy [110], S. Roy [49], N. Rubini [25],
O.V. Rueda [81], D. Ruggiano [143], R. Rui [23], B. Rumyantsev [75], P.G. Russek [2], R. Russo [91], A. Rustamov [88],
E. Ryabinkin [89], Y. Ryabov [99], A. Rybicki [118], H. Rytkonen [126], W. Rzesa [143], O.A.M. Saarimaki [44],
R. Sadek [115], S. Sadovsky [92], J. Saetre [21], K. Šafařík [37], S.K. Saha [142], S. Saha [87], B. Sahoo [49], P. Sahoo [49],
R. Sahoo [50], S. Sahoo [65], D. Sahu [50], P.K. Sahu [65], J. Saini [142], S. Sakai [134], M.P. Salvan [108], S. Sambyal [102],
T.B. Saramela [121], D. Sarkar [144], N. Sarkar [142], P. Sarma [42], V.M. Sarti [106], M.H.P. Sas [147], J. Schambach [97],
H.S. Scheid [68], C. Schiaua [48], R. Schicker [105], A. Schmah [105], C. Schmidt [108], H.R. Schmidt [104],
M.O. Schmidt [34,105], M. Schmidt [104], N.V. Schmidt [97,68], A.R. Schmier [131], R. Schotter [138], J. Schukraft [34],
K. Schwarz [108], K. Schweda [108], G. Scioli [25], E. Scomparin [59], J.E. Seger [15], Y. Sekiguchi [133], D. Sekihata [133],
I. Selyuzhenkov [108,94], S. Senyukov [138], J.J. Seo [61], D. Serebryakov [63], L. Šerkšnytė [106], A. Sevcenco [67],
T.J. Shaba [72], A. Shabanov [63], A. Shabetai [115], R. Shahoyan [34], W. Shaikh [110], A. Shangaraev [92],

A. Sharma [101], H. Sharma [118], M. Sharma [102], N. Sharma [101], S. Sharma [102], U. Sharma [102], A. Shatat [78], O. Sheibani [125], K. Shigaki [46], M. Shimomura [84], S. Shirinkin [93], Q. Shou [40], Y. Sibiriak [89], S. Siddhanta [55], T. Siemiarczuk [86], T.F. Silva [121], D. Silvermyr [81], T. Simantathammakul [116], G. Simonetti [34], B. Singh [106], R. Singh [87], R. Singh [102], R. Singh [50], V.K. Singh [142], V. Singhal [142], T. Sinha [110], B. Sitar [13], M. Sitta [31], T.B. Skaali [20], G. Skorodumovs [105], M. Slupecki [44], N. Smirnov [147], R.J.M. Snellings [62], C. Soncco [112], J. Song [125], A. Songmoolnak [116], F. Soramel [27], S. Sorensen [131], I. Sputowska [118], J. Stachel [105], I. Stan [67], P.J. Steffanic [131], S.F. Stiefelmaier [105], D. Stocco [115], I. Storehaug [20], M.M. Storetvedt [36], P. Stratmann [145], S. Strazzi [25], C.P. Stylianidis [91], A.A.P. Suaide [121], C. Suire [78], M. Sukhanov [63], M. Suljic [34], R. Sultanov [93], V. Sumberia [102], S. Sumowidagdo [51], S. Swain [65], A. Szabo [13], I. Szarka [13], U. Tabassam [14], S.F. Taghavi [106], G. Taillepied [108,136], J. Takahashi [122], G.J. Tambave [21], S. Tang [136,7], Z. Tang [129], J.D. Tapia Takaki [127,VII], N. Tapus [135], M.G. Tarzila [48], A. Tauro [34], G. Tejeda Muñoz [45], A. Telesca [34], L. Terlizzi [24], C. Terrevoli [125], G. Tersimonov [3], S. Thakur [142], D. Thomas [119], R. Tieulent [137], A. Tikhonov [63], A.R. Timmins [125], M. Tkacik [117], A. Toia [68], N. Topilskaya [63], M. Toppi [52], F. Torales-Acosta [19], T. Tork [78], A. Trifiró [32,56], A.S. Triolo [32], S. Tripathy [54,69], T. Tripathy [49], S. Trogolo [34,27], V. Trubnikov [3], W.H. Trzaska [126], T.P. Trzcinski [143], A. Tumkin [109], R. Turrisi [57], T.S. Tveter [20], K. Ullaland [21], A. Uras [137], M. Urioni [58,141], G.L. Usai [22], M. Vala [38], N. Valle [28], S. Vallero [59], L.V.R. van Doremalen [62], M. van Leeuwen [91], R.J.G. van Weelden [91], P. Vande Vyvre [34], D. Varga [146], Z. Varga [146], M. Varga-Kofarago [146], M. Vasileiou [85], A. Vasiliev [89], O. Vázquez Doce [52,106], V. Vechernin [113], A. Velure [21], E. Vercellin [24], S. Vergara Limón [45], L. Vermunt [62], R. Vértesi [146], M. Verweij [62], L. Vickovic [35], Z. Vilakazi [132], O. Villalobos Baillie [111], G. Vino [53], A. Vinogradov [89], T. Virgili [29], V. Vislavicius [90], A. Vodopyanov [75], B. Volkel [34,105], M.A. Völkl [105], K. Voloshin [93], S.A. Voloshin [144], G. Volpe [33], B. von Haller [34], I. Vorobyev [106], N. Vozniuk [63], J. Vrláková [38], B. Wagner [21], C. Wang [40], D. Wang [40], M. Weber [114], A. Wegrzynek [34], S.C. Wenzel [34], J.P. Wessels [145], S.L. Weyhmiller [147], J. Wiechula [68], J. Wikne [20], G. Wilk [86], J. Wilkinson [108], G.A. Willems [145], B. Windelband [105], M. Winn [139], W.E. Witt [131], J.R. Wright [119], W. Wu [40], Y. Wu [129], R. Xu [7], A.K. Yadav [142], S. Yalcin [77], Y. Yamaguchi [46], K. Yamakawa [46], S. Yang [21], S. Yano [46], Z. Yin [7], I.-K. Yoo [17], J.H. Yoon [61], S. Yuan [21], A. Yuncu [105], V. Zaccolo [23], C. Zampolli [34], H.J.C. Zanoli [62], F. Zanone [105], N. Zardoshti [34], A. Zarochentsev [113], P. Závada [66], N. Zaviyalov [109], M. Zhalov [99], B. Zhang [7], S. Zhang [40], X. Zhang [7], Y. Zhang [129], V. Zherebchevskii [113], Y. Zhi [11], N. Zhigareva [93], D. Zhou [7], Y. Zhou [90], J. Zhu [108,7], Y. Zhu [7], G. Zinovjev [3,I], N. Zurlo [141,58]

[1] A.I. Alikhanyan National Science Laboratory (Yerevan Physics Institute) Foundation, Yerevan, Armenia
[2] AGH University of Science and Technology, Cracow, Poland
[3] Bogolyubov Institute for Theoretical Physics, National Academy of Sciences of Ukraine, Kiev, Ukraine
[4] Bose Institute, Department of Physics and Centre for Astroparticle Physics and Space Science (CAPSS), Kolkata, India
[5] Budker Institute for Nuclear Physics, Novosibirsk, Russia
[6] California Polytechnic State University, San Luis Obispo, CA, United States
[7] Central China Normal University, Wuhan, China
[8] Centro de Aplicaciones Tecnológicas y Desarrollo Nuclear (CEADEN), Havana, Cuba
[9] Centro de Investigación y de Estudios Avanzados (CINVESTAV), Mexico City and Mérida, Mexico
[10] Chicago State University, Chicago, IL, United States
[11] China Institute of Atomic Energy, Beijing, China
[12] Chungbuk National University, Cheongju, Republic of Korea
[13] Comenius University Bratislava, Faculty of Mathematics, Physics and Informatics, Bratislava, Slovakia
[14] COMSATS University Islamabad, Islamabad, Pakistan
[15] Creighton University, Omaha, NE, United States
[16] Department of Physics, Aligarh Muslim University, Aligarh, India
[17] Department of Physics, Pusan National University, Pusan, Republic of Korea
[18] Department of Physics, Sejong University, Seoul, Republic of Korea
[19] Department of Physics, University of California, Berkeley, CA, United States
[20] Department of Physics, University of Oslo, Oslo, Norway
[21] Department of Physics and Technology, University of Bergen, Bergen, Norway
[22] Dipartimento di Fisica dell'Università and Sezione INFN, Cagliari, Italy
[23] Dipartimento di Fisica dell'Università and Sezione INFN, Trieste, Italy
[24] Dipartimento di Fisica dell'Università and Sezione INFN, Turin, Italy
[25] Dipartimento di Fisica e Astronomia dell'Università and Sezione INFN, Bologna, Italy
[26] Dipartimento di Fisica e Astronomia dell'Università and Sezione INFN, Catania, Italy
[27] Dipartimento di Fisica e Astronomia dell'Università and Sezione INFN, Padova, Italy
[28] Dipartimento di Fisica e Nucleare e Teorica, Università di Pavia, Pavia, Italy
[29] Dipartimento di Fisica 'E.R. Caianiello' dell'Università and Gruppo Collegato INFN, Salerno, Italy
[30] Dipartimento DISAT del Politecnico and Sezione INFN, Turin, Italy
[31] Dipartimento di Scienze e Innovazione Tecnologica dell'Università del Piemonte Orientale and INFN Sezione di Torino, Alessandria, Italy
[32] Dipartimento di Scienze MIFT, Università di Messina, Messina, Italy
[33] Dipartimento Interateneo di Fisica 'M. Merlin' and Sezione INFN, Bari, Italy
[34] European Organization for Nuclear Research (CERN), Geneva, Switzerland
[35] Faculty of Electrical Engineering, Mechanical Engineering and Naval Architecture, University of Split, Split, Croatia
[36] Faculty of Engineering and Science, Western Norway University of Applied Sciences, Bergen, Norway

37 *Faculty of Nuclear Sciences and Physical Engineering, Czech Technical University in Prague, Prague, Czech Republic*
38 *Faculty of Science, P.J. Šafárik University, Košice, Slovakia*
39 *Frankfurt Institute for Advanced Studies, Johann Wolfgang Goethe-Universität Frankfurt, Frankfurt, Germany*
40 *Fudan University, Shanghai, China*
41 *Gangneung-Wonju National University, Gangneung, Republic of Korea*
42 *Gauhati University, Department of Physics, Guwahati, India*
43 *Helmholtz-Institut für Strahlen- und Kernphysik, Rheinische Friedrich-Wilhelms-Universität Bonn, Bonn, Germany*
44 *Helsinki Institute of Physics (HIP), Helsinki, Finland*
45 *High Energy Physics Group, Universidad Autónoma de Puebla, Puebla, Mexico*
46 *Hiroshima University, Hiroshima, Japan*
47 *Hochschule Worms, Zentrum für Technologietransfer und Telekommunikation (ZTT), Worms, Germany*
48 *Horia Hulubei National Institute of Physics and Nuclear Engineering, Bucharest, Romania*
49 *Indian Institute of Technology Bombay (IIT), Mumbai, India*
50 *Indian Institute of Technology Indore, Indore, India*
51 *Indonesian Institute of Sciences, Jakarta, Indonesia*
52 *INFN, Laboratori Nazionali di Frascati, Frascati, Italy*
53 *INFN, Sezione di Bari, Bari, Italy*
54 *INFN, Sezione di Bologna, Bologna, Italy*
55 *INFN, Sezione di Cagliari, Cagliari, Italy*
56 *INFN, Sezione di Catania, Catania, Italy*
57 *INFN, Sezione di Padova, Padova, Italy*
58 *INFN, Sezione di Pavia, Pavia, Italy*
59 *INFN, Sezione di Torino, Turin, Italy*
60 *INFN, Sezione di Trieste, Trieste, Italy*
61 *Inha University, Incheon, Republic of Korea*
62 *Institute for Gravitational and Subatomic Physics (GRASP), Utrecht University/Nikhef, Utrecht, Netherlands*
63 *Institute for Nuclear Research, Academy of Sciences, Moscow, Russia*
64 *Institute of Experimental Physics, Slovak Academy of Sciences, Košice, Slovakia*
65 *Institute of Physics, Homi Bhabha National Institute, Bhubaneswar, India*
66 *Institute of Physics of the Czech Academy of Sciences, Prague, Czech Republic*
67 *Institute of Space Science (ISS), Bucharest, Romania*
68 *Institut für Kernphysik, Johann Wolfgang Goethe-Universität Frankfurt, Frankfurt, Germany*
69 *Instituto de Ciencias Nucleares, Universidad Nacional Autónoma de México, Mexico City, Mexico*
70 *Instituto de Física, Universidade Federal do Rio Grande do Sul (UFRGS), Porto Alegre, Brazil*
71 *Instituto de Física, Universidad Nacional Autónoma de México, Mexico City, Mexico*
72 *iThemba LABS, National Research Foundation, Somerset West, South Africa*
73 *Jeonbuk National University, Jeonju, Republic of Korea*
74 *Johann-Wolfgang-Goethe Universität Frankfurt Institut für Informatik, Fachbereich Informatik und Mathematik, Frankfurt, Germany*
75 *Joint Institute for Nuclear Research (JINR), Dubna, Russia*
76 *Korea Institute of Science and Technology Information, Daejeon, Republic of Korea*
77 *KTO Karatay University, Konya, Turkey*
78 *Laboratoire de Physique des 2 Infinis, Irène Joliot-Curie, Orsay, France*
79 *Laboratoire de Physique Subatomique et de Cosmologie, Université Grenoble-Alpes, CNRS-IN2P3, Grenoble, France*
80 *Lawrence Berkeley National Laboratory, Berkeley, CA, United States*
81 *Lund University Department of Physics, Division of Particle Physics, Lund, Sweden*
82 *Moscow Institute for Physics and Technology, Moscow, Russia*
83 *Nagasaki Institute of Applied Science, Nagasaki, Japan*
84 *Nara Women's University (NWU), Nara, Japan*
85 *National and Kapodistrian University of Athens, School of Science, Department of Physics, Athens, Greece*
86 *National Centre for Nuclear Research, Warsaw, Poland*
87 *National Institute of Science Education and Research, Homi Bhabha National Institute, Jatni, India*
88 *National Nuclear Research Center, Baku, Azerbaijan*
89 *National Research Centre Kurchatov Institute, Moscow, Russia*
90 *Niels Bohr Institute, University of Copenhagen, Copenhagen, Denmark*
91 *Nikhef, National institute for subatomic physics, Amsterdam, Netherlands*
92 *NRC Kurchatov Institute IHEP, Protvino, Russia*
93 *NRC «Kurchatov»Institute – ITEP, Moscow, Russia*
94 *NRNU Moscow Engineering Physics Institute, Moscow, Russia*
95 *Nuclear Physics Group, STFC Daresbury Laboratory, Daresbury, United Kingdom*
96 *Nuclear Physics Institute of the Czech Academy of Sciences, Řež u Prahy, Czech Republic*
97 *Oak Ridge National Laboratory, Oak Ridge, TN, United States*
98 *Ohio State University, Columbus, OH, United States*
99 *Petersburg Nuclear Physics Institute, Gatchina, Russia*
100 *Physics department, Faculty of science, University of Zagreb, Zagreb, Croatia*
101 *Physics Department, Panjab University, Chandigarh, India*
102 *Physics Department, University of Jammu, Jammu, India*
103 *Physics Department, University of Rajasthan, Jaipur, India*
104 *Physikalisches Institut, Eberhard-Karls-Universität Tübingen, Tübingen, Germany*
105 *Physikalisches Institut, Ruprecht-Karls-Universität Heidelberg, Heidelberg, Germany*
106 *Physik Department, Technische Universität München, Munich, Germany*
107 *Politecnico di Bari and Sezione INFN, Bari, Italy*
108 *Research Division and ExtreMe Matter Institute EMMI, GSI Helmholtzzentrum für Schwerionenforschung GmbH, Darmstadt, Germany*
109 *Russian Federal Nuclear Center (VNIIEF), Sarov, Russia*
110 *Saha Institute of Nuclear Physics, Homi Bhabha National Institute, Kolkata, India*
111 *School of Physics and Astronomy, University of Birmingham, Birmingham, United Kingdom*
112 *Sección Física, Departamento de Ciencias, Pontificia Universidad Católica del Perú, Lima, Peru*
113 *St. Petersburg State University, St. Petersburg, Russia*
114 *Stefan Meyer Institut für Subatomare Physik (SMI), Vienna, Austria*
115 *SUBATECH, IMT Atlantique, Université de Nantes, CNRS-IN2P3, Nantes, France*
116 *Suranaree University of Technology, Nakhon Ratchasima, Thailand*

[117] Technical University of Košice, Košice, Slovakia
[118] The Henryk Niewodniczanski Institute of Nuclear Physics, Polish Academy of Sciences, Cracow, Poland
[119] The University of Texas at Austin, Austin, TX, United States
[120] Universidad Autónoma de Sinaloa, Culiacán, Mexico
[121] Universidade de São Paulo (USP), São Paulo, Brazil
[122] Universidade Estadual de Campinas (UNICAMP), Campinas, Brazil
[123] Universidade Federal do ABC, Santo Andre, Brazil
[124] University of Cape Town, Cape Town, South Africa
[125] University of Houston, Houston, TX, United States
[126] University of Jyväskylä, Jyväskylä, Finland
[127] University of Kansas, Lawrence, KS, United States
[128] University of Liverpool, Liverpool, United Kingdom
[129] University of Science and Technology of China, Hefei, China
[130] University of South-Eastern Norway, Tonsberg, Norway
[131] University of Tennessee, Knoxville, TN, United States
[132] University of the Witwatersrand, Johannesburg, South Africa
[133] University of Tokyo, Tokyo, Japan
[134] University of Tsukuba, Tsukuba, Japan
[135] University Politehnica of Bucharest, Bucharest, Romania
[136] Université Clermont Auvergne, CNRS/IN2P3, LPC, Clermont-Ferrand, France
[137] Université de Lyon, CNRS/IN2P3, Institut de Physique des 2 Infinis de Lyon, Lyon, France
[138] Université de Strasbourg, CNRS, IPHC UMR 7178, F-67000 Strasbourg, France
[139] Université Paris-Saclay Centre d'Etudes de Saclay (CEA), IRFU, Département de Physique Nucléaire (DPhN), Saclay, France
[140] Università degli Studi di Foggia, Foggia, Italy
[141] Università di Brescia, Brescia, Italy
[142] Variable Energy Cyclotron Centre, Homi Bhabha National Institute, Kolkata, India
[143] Warsaw University of Technology, Warsaw, Poland
[144] Wayne State University, Detroit, MI, United States
[145] Westfälische Wilhelms-Universität Münster, Institut für Kernphysik, Münster, Germany
[146] Wigner Research Centre for Physics, Budapest, Hungary
[147] Yale University, New Haven, Connecticut, United States
[148] Yonsei University, Seoul, Republic of Korea

[I] Deceased.
[II] Also at: Italian National Agency for New Technologies, Energy and Sustainable Economic Development (ENEA), Bologna, Italy.
[III] Also at: Dipartimento DET del Politecnico di Torino, Turin, Italy.
[IV] Also at: M.V. Lomonosov Moscow State University, D.V. Skobeltsyn Institute of Nuclear, Physics, Moscow, Russia.
[V] Also at: Department of Applied Physics, Aligarh Muslim University, Aligarh, India.
[VI] Also at: Institute of Theoretical Physics, University of Wroclaw, Poland.
[VII] Also at: University of Kansas, Lawrence, Kansas, United States.